



[bresson.emilie@ouranos.ca]

# Bias-adjusted projections of snow cover over eastern Canada using an ensemble of regional climate models

Émilie Bresson<sup>1</sup>, Éric Dupuis<sup>1</sup>, and Pascal Bourgault<sup>1</sup>

<sup>1</sup>Ouranos Inc., 550 Rue Sherbrooke W., West Tower, 19<sup>th</sup> floor, Montreal, Québec, H3A 1B9, Canada

**Abstract.** In the context of climate change, stakeholders and decision makers need easily accessible bias-adjusted projections of snow cover and indices produced from those to develop adaptation plans. To meet this need, we produced an ensemble of regional climate projections statistically bias adjusted of snow water equivalent (SWE) in the province of Québec, Canada. This bias adjustment required some fine-tuning to operational methods, mainly due to the seasonality in the SWE. We calculated indices of interest for several sectors based on the bias-adjusted SWE. These indices included the maximum of SWE as well as the duration, start, and end of the snow season, and the days without snow cover. In eastern Canada, snow cover tended to persist for shorter periods as the climate warms, with symmetrical shrinkage at the beginning and the end of the snow season, with the exception of the Nunavik region. The maximum SWE was projected to decrease in the southern part of the domain and increase elsewhere. The snow season in the Côte-Nord, southern Québec and St-Lawrence River Valley regions would be increasingly interrupted by sequences of days without snow cover, whereas this would not be the case for the northern and central Québec regions.

## 1 Introduction

Changes in snow cover have a significant feedback on climate, specifically in the northern part of the northern hemisphere, which witnesses a decrease in snow cover extent, a shortening of the snow season (Derksen et al., 2019; McCrary et al., 2022; Mudryk et al., 2020; Fox-Kemper et al., 2021) and a greater warming than in the rest of the world (e.g. Hoegh-Guldberg et al., 2018). These changes in snow cover affect water supply (e.g. Mankin et al., 2015), agriculture (e.g. Bélanger et al., 2002), ecology (e.g. Zimova et al., 2016), hydroelectricity or flooding through streamflow changes (e.g. Dudley et al., 2017; Arora et al., 2025), tourism (e.g. Scott et al., 2020) etc. Stakeholders and decision makers need accurate climate information to adapt to climate change. The widespread practice in climate services is to adjust the bias of global climate simulations and combine them in an ensemble to provide ensemble statistics (Lavoie et al., 2024). Currently, this is usually only applied to the best understood variables, namely surface temperature and precipitation (e.g. Climate Portraits, climatedata.ca, Climate Atlas of Copernicus). Several climate indices are derived from these bias-adjusted variables. Extending the scope of these bias-adjusted datasets can be challenging. Some variables such as freezing rain have rare occurrences; Other variables such as snow on the ground or precipitations in regions with a monsoon regime exhibit strong seasonality. These features are difficult to handle with standard bias adjustment techniques.



The snow cover variables such as snow depth or snow water equivalent are simulated by land surface models (LSMs), such as CROCUS (Brun et al., 2013), CLASS/CLASSIC (Melton et al., 2020; Verseghy, 1991), or HTESSEL (Dutra et al., 2009). Each LSM has its pros and cons (e.g. Lee et al., 2024). The LSMs can be used coupled with the atmosphere in a global (GCM) or regional (RCM) climate model. Users can then work with the snow data produced by a climate model coupled to a LSM and such data are already available through projects like CMIP6, but this option has drawbacks, as the raw models have a coarse resolution and their biases have not been addressed. LSMs can also be used in an offline-mode, which presents some advantages, like allowing a higher resolution to better reproduce the surface and the processes such as sublimation or ablation, as these models are cheaper to run than coupled climate models. Consequently, this method could be better adapted for specific purposes at a local scale (e.g. Morin et al., 2021). However, no feedback between the surface and the atmosphere is then allowed, and the local scale limits a broader use of the data.

To the best of our knowledge, these are the two possibilities to work with snow depth or SWE projections (LSM coupled to a GCM or RCM, and LSM in offline-mode). On the other hand, different users need accurate climate information with a high resolution in a large domain. To fill the gap between supply and demand, we propose to generate and give access to an ensemble of bias-adjusted snow cover indicators based on snow data produced by RCMs with an horizontal resolution of  $0.1^\circ$ . This will make use of the RCMs' advantages: finer resolution than GCMs, coupled LSM, large domain for wide applicability. In terms of bias adjustment methods, some have been applied to snowpack characteristics (Matiu and Hanzer, 2022), but these methods were exclusively considered for the snow cover. To our knowledge, there is only one bias adjustment method that has been successfully applied to the snow amount, or snow water equivalent (Michel et al., 2023). We propose using this method to bias-adjust the SWE data. Furthermore, snow cover indices will be computed based on the bias-adjusted SWE. The choice of the variable (SWE instead of snow depth) allows us to focus on the water content in the snowpack, which, contrary to snow depth, is independent of the snow density. We produced the SWE indices for a domain including the Canadian province of Québec (eastern Canada). This domain has mountains of medium altitude, which alleviates problems often arising with snow simulation in high-altitude terrain such as the Rocky Mountains (e.g. McCrary et al., 2022; Kouki et al., 2022; Santolaria-Otín and Zolina, 2020).

This article is organized as follows. Sect. 2 presents the data, methods and domains used to produce the snow cover indices ensemble, which is then analyzed in Sect. 3. Discussion follows in Sect. 4 before a conclusion (Sect. 5).

## 2 Data and Methods

### 2.1 Domain and regions of interest

The study covered the Canadian province of Québec (Fig. 1). Five smaller regions ( $10 \times 10$  grid points, that is,  $1^\circ \times 1^\circ$ ) were defined to present a climatic diversity (Fig. 1). The southern, central and northern Québec domains followed a North-South transect along the same longitude to investigate the meridional gradient. The effect of an altitude gradient was studied by comparing the plains in the St-Lawrence River Valley (SLRV) with southern Québec, as these domains share a similar latitude range but the former region is at lower altitudes. Comparison between a domain with more oceanic influence (Côte-Nord)

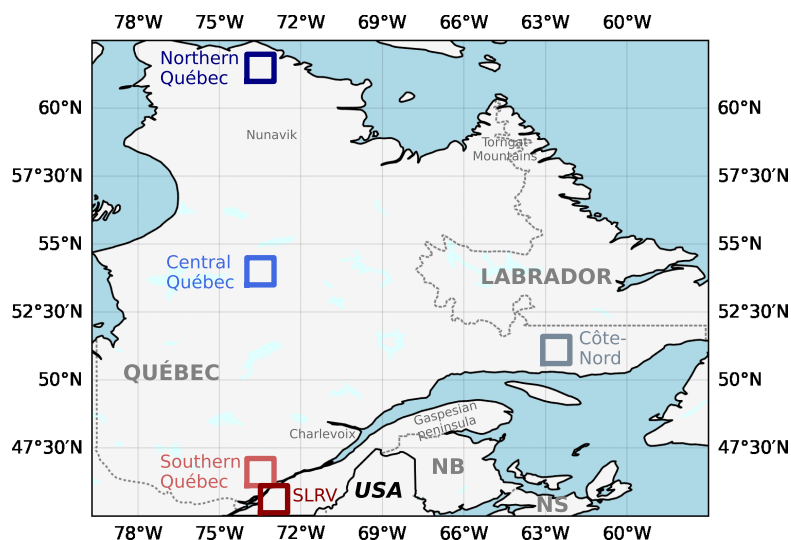


**Figure 1.** Studied domains. Boxes outline the following regions: northern Québec (dark blue), central Québec (blue), Côte-Nord (grey), southern Québec (light red) and St-Lawrence River Valley (SLRV; brown). NB: New Brunswick; NS: Nova Scotia.

60 and a continental domain (central Québec) was also considered. These domains are represented by colored boxes in Fig. 1: northern Québec (dark blue), central Québec (blue), Côte-Nord (gray), southern Québec (light red) and St-Lawrence River Valley (SLRV; brown). Results presented for these regions correspond to the spatial mean within the area.

## 2.2 Snow cover indices

Several indices were studied to describe the behaviour of the snow cover: Start (SSS), End (SSE) and Duration (SSD) of the snow season; Annual maximum SWE (SWEmax); Days without snow cover (noSC). Their characteristics are specified in Table 1. Snow cover was defined as a  $SWE \geq 4$  mm (Mudryk et al., 2017), consequently noSC was defined as days with  $SWE < 4$  mm. SSS was the first day of the first 14 consecutive days with snow cover, and SSE was the first day, after SSS, without snow cover for 14 consecutive days. The snow season duration was simply the number of days between those dates. Note that the snow season can include days without snow cover, as long the 14 day streak is not reached. The 14 day threshold was chosen for two reasons: it was long enough to avoid an artificially short snow season when the snow cover is often interrupted by brief warm spells, and it was short enough to allow some flexibility in the determination of SSS and SSE, in opposition to a 30 day threshold like the one used in Brown (2010). Indices were calculated annually for winter years, starting on August 1<sup>st</sup> and ending on July 31<sup>st</sup>. They were calculated on statistically bias-adjusted SWE timeseries from an ensemble of RCM simulations described in the next section.

75 For analysis purposes, another indicator, noSCseq, was defined in order to investigate the fragmentation of the snow cover. noSCseq looks at sequences of 2 to 13 consecutive days without snow cover (days with  $SWE < 4$  mm). We chose a limit of



**Table 1.** List of snow cover indices characteristics (name, definition, unit).

Name	Definition	Unit
SWEmax	Annual maximum SWE	mm
SSS	Snow season start: first date on which SWE $\geq 4$ mm for 14 consecutive days	day of year
SSE	Snow season end: first date (after SSS) on which SWE $< 4$ mm for 14 consecutive days	day of year
SSD	Snow season duration: number of days between SSS and SSE	days
noSC	Number of days without snow cover (days with SWE $< 4$ mm)	days

13 consecutive days for noSCseq in order to consider only the period during which a snow cover could be present, since our threshold for the snow season start [end] is 14 consecutive days with [without] snow on the ground (Tab. 1). We found all such sequences for all regions and for each periods of 30 years. We grouped these by the day of year on which they start and took the 30 years mean of their length, which enabled us to obtain climatological data on the duration of noSCseq starting on each day of the year in each region for different horizons. Finally, as described in Sect. 2.1, spatial mean within the area was performed for each region.

## 2.3 Data

### 2.3.1 Reference data

For this study, the historical period (1991–2020) was defined as August 1, 1991 to July 31, 2021. We considered reference data that provided daily SWE data on a high-resolution grid with a coverage of the historical period and that demonstrated good performance over the Québec domain. Several SWE gridded databases were available like ERA5, ERA5-Land, MERRA-2 or B-TIM products (Mudryk et al., 2015, 2024; Mortimer et al., 2024; Mudryk et al., 2017; Hersbach et al., 2020; Muñoz-Sabater et al., 2021; Molod et al., 2015; Elias Chereque et al., 2024). However, a mismatch was observed between these databases. Studying the northern hemisphere, Mudryk et al. (2015) highlighted that the spread in climatological values was mainly due to the different land surface models simulating the snow water mass in the reanalysis products. Kanda and Fletcher (2025) analyzed the bias of ERA5-Land SWE for Northern Canada (above the 50th parallel north) against CanSWE observations (Vionnet et al., 2021), for three ranges of elevation. In Québec, the selected stations belonged in either low or medium elevation categories. In their results, they highlighted that ERA5-Land tends to underestimate large snow-packs (exceeding 300 mm, mainly high-altitude stations), well-estimate mid-elevation regions and underestimate low-elevation regions. Nevertheless, Mudryk et al. (2024) showed that ERA5-Land had a good SWE performance for eastern North America among over products and the ERA5-Land product was selected as the reference data for this study. This database was produced by a land surface model running offline and driven by ERA5 atmospheric fields. ERA5-Land has a 0.1 ° horizontal resolution and an hourly temporal resolution and its SWE data is publicly available (named “snow depth water equivalent”).



### 100 2.3.2 RCM Simulations Ensemble

The list of mandatory archived variables for the Coordinated Regional Climate Downscaling Experiment (CORDEX; Giorgi et al., 2009) did not include SWE; Only certain modelling institutions archived and shared their SWE data. This led to a preliminary simulation ensemble encompassing only a subset of the simulations produced through the North America CORDEX (NA-CORDEX Mearns et al.) project, to which several additional simulations from the CRCM5 (5<sup>th</sup> generation of the Canadian Regional Climate Model; Martynov et al., 2013; Šeparović et al., 2013) ran at Ouranos were added (SM).

A first scan of the simulated SWE showed large discrepancies, as already highlighted in the literature (e.g. McCrary et al., 2022), forcing a selection of simulations to build the ensemble. Indeed, to perform a statistical bias adjustment on a variable with a strong annual cycle like SWE, a good synchronization in the timing of the thaw and accumulation periods is needed. Specifically, a simulation with a short snow seasons bias posed challenges, as the longer sequences without snow cover could have not been adjusted with usual multiplicative methods. Indeed, common statistical bias adjustment methods do not adjust the seasonality of variables explicitly and won't perform well for a variable that is exactly zero for long stretches of time, such as SWE.

A selection of simulations was thus required, and this was a limitation for the kind of simple bias-adjustment method that was prioritized. This process was performed keeping in mind the fragile balance between having the best performing simulations and keeping an ensemble large enough to cover uncertainties of different emission scenarios and RCMs. The selection criteria were based on the SSS and SSE indices described above, and focused on the southern part of the domain ( $< 50^\circ$  N) where most observations were available and where gridded products usually performed better (e.g. Vionnet et al., 2021; Mudryk et al., 2017). A simulation was kept if, for more than 80 % of the target grid-points, the SSS bias did not exceed 10 days and SSE bias did not exceed 15 days. The final ensemble included 10 simulations (Tab. 2) and was compared with results from McCrary et al. (2022) to attest the coherence between their findings and ours. In their study, they rejected simulations from the RegCM4 RCM as it did not perform well enough in western North America. Our region of interest was not affected by this poor performance and a simulation produced with the RegCM4 RCM was considered, as it met the previous criteria.

### 2.4 Bias-adjustment Method

Statistical methods based on the adjustment of marginals can be limited in their ability to correct SWE time series. Since SWE is a variable bounded by 0 (a ratio variable), it is common to use multiplicative adjustment factors for each quantile when using quantile-mapping-based methods. This guarantees that SWE remains positive. However, if a simulation is biased and, for example, the end of its snow season (i.e., when the snow cover has totally melted) is too early in the year, then multiplying 0 with an adjustment factor will not correct the lack of snow.

A similar phenomenon can occur for precipitation, when the source distribution has a higher frequency of dry days than its target. In this instance, small values of precipitation can be randomly dispersed throughout the source time series to address this issue and help with the adjustment (Thiemeßl et al., 2012). In the case of SWE, the problematic values occur in consecutive days of the year. Changing a large fraction of these zeroes is then more delicate, as it would effectively prescribe a synchronous



**Table 2.** Ensemble of simulations considered in this paper. Simulation names correspond to Driving-GCM\_RCM\_RCM-Institution. More details can be found in SM.

Simulation name	RCP4.5	RCP8.5
CNRM-CM5_CRCM5_OURANOS	X	X
GFDL-ESM2M_CRCM5_OURANOS	X	X
GFDL-ESM2M_WRF_NCAR		X
MOHC-HadGEM2-ES_RegCM4_ISU		X
MPI-ESM-LR_CRCM5_OURANOS	X	X
MPI-ESM-LR_CRCM5_UQAM	X	
MPI-ESM-LR_RegCM4_NCAR		X

adjustment of the time series. In the case of precipitation just mentioned, the pre-processing is rather statistical in nature, and simply precedes more statistical adjustments.

135 A method to tackle this issue was proposed in Michel et al. (2023) and was based on simple Empirical Quantile Mapping (QM) (Cannon et al., 2015) supplemented with a pre-processing of the SWE time series. Declines of SWE were smoothed with an exponential decay by replacing vanishing values with the preceding value divided by two. A minimal threshold of SWE (set to  $0.5 \text{ mm d}^{-1}$  in Michel et al., 2023) was then set, below which values were set to 0. The end of a snow season is mainly controlled by the melting mechanism, which was safer to extrapolate than the snow fall. In this study, we used a  
 140 smaller threshold  $0.001 \text{ mm}$  to keep more non-zero SWE data points reinserted by the decay process, but we performed this reinsertion in a limited time period: We restricted the decay process to data points near the snow season end, but defined with a  $1 \text{ mm}$  threshold for this purpose (instead of  $4 \text{ mm}$ ). Hence, abnormal negligible snowfalls later in the year were not modified with new decaying values of SWE.

The reference period for the bias adjustment was the historical period 1991–2020.

## 145 3 Results

### 3.1 Snow cover climatology

During the historical period (1991–2020), SWE<sub>max</sub> was larger over the eastern part of Québec and Labrador (e.g.  $375 \text{ mm}$  for Côte-Nord), and particularly over mountainous regions like the Gaspesian peninsula, Charlevoix, or the Torngat Mountains than the rest of the domain (e.g.  $216 \text{ mm}$  for central Québec) (Fig. 2a). The plains in the south of the domain (SLRV) showed  
 150 the smallest maximum SWE ( $107 \text{ mm}$ ), about  $100 \text{ mm}$  less than the mountainous region at a similar latitude (southern Québec region). Meanwhile, a South-North gradient is noticeable for SSD, SSS, SSE and noSC (Fig. 2d,g, 3a). For example, the northern Québec region experienced long SSD ( $273 \text{ days}$ ), few noSC ( $90 \text{ days}$ ) (Fig. 2d,g), and had a snow season that began



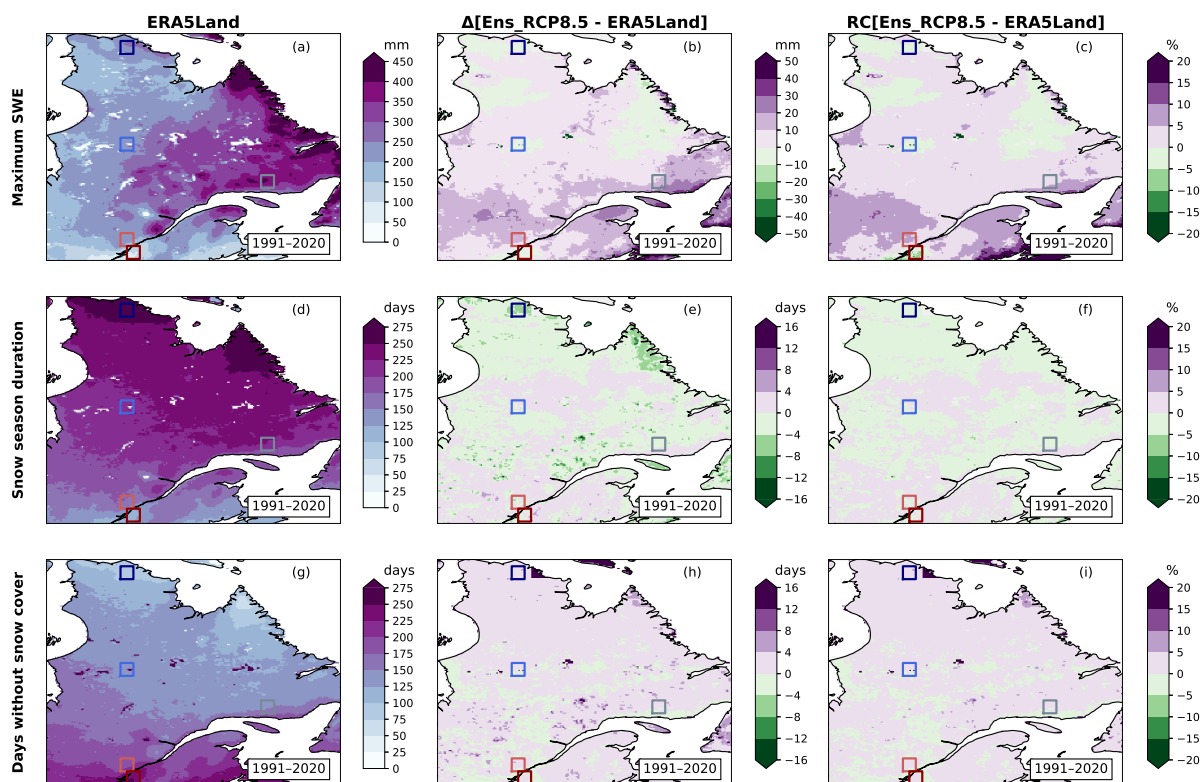


**Figure 2.** Annual maximum SWE (first row), snow season duration (second row) and days without snow cover (third row) for ERA5-Land (left), difference (middle) and relative change (right) between the RCP8.5 ensemble and ERA5-Land for the 1991–2020 period.

late September and ended late June (Fig. 3a). In comparison, the southern Québec region had a short snow season (SSD; 166 days), starting in mid-November and ending in early May, and 196 days without snow cover (noSC) (Fig. 2d,g, 3a). This meridional gradient was also observed when looking at the date when the maximum of SWE happens: from mid-May in northern Québec to late March in southern Québec (Fig. 5a,b,d).

In general, the RCP4.5 and RCP8.5 ensembles presented the same portrait for all indices on the historical period (Fig. 2b,e,h,k, 3b, SM). Relative biases of the ensembles compared with ERA5-Land are globally  $\pm 5\%$  for SWEmax, SSD and noSC indices (Fig. 2c,f,i,l, SM). In the southern part of the domain, the positive bias reached 10 to 15 % for SWEmax (Fig. 2c).

## 3.2 Projected changes in snow cover

The future periods studied hereafter are 2041–2070 (August 1, 2041–July 31, 2071) and 2070–2099 (August 1, 2070–July 31, 2100). The two RCP ensembles presented similar trends, but the magnitude of change was smaller for the RCP4.5 experiment than for RCP8.5. Only the results of the RCP8.5 were presented here to streamline the text. The results for the RCP4.5 ensemble are available in the supplemental material (SM).

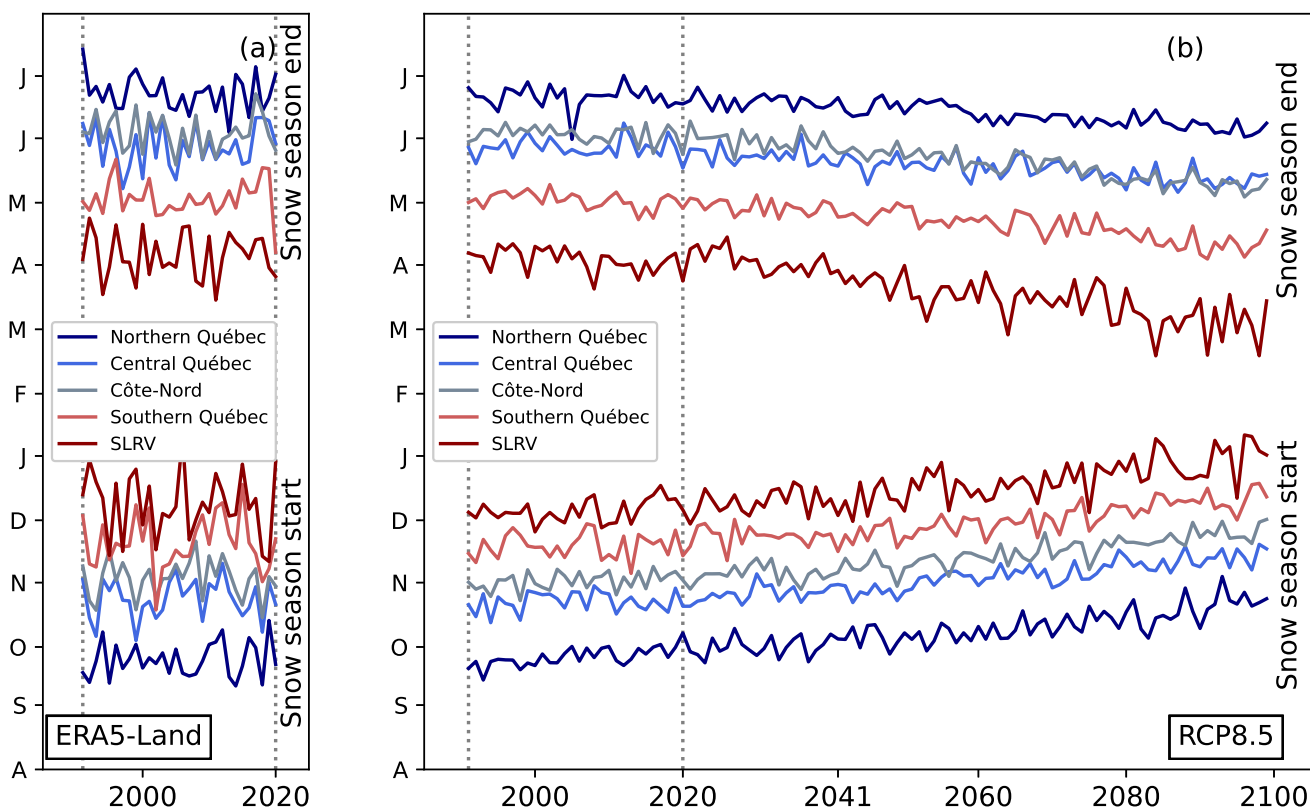


**Figure 3.** Time series of snow season start (bottom) and snow season end (top) for ERA5-Land (a) and the RCP8.5 ensemble (b) for the five regions of interest. Dashed gray vertical lines encompass the historical period (1991–2020).

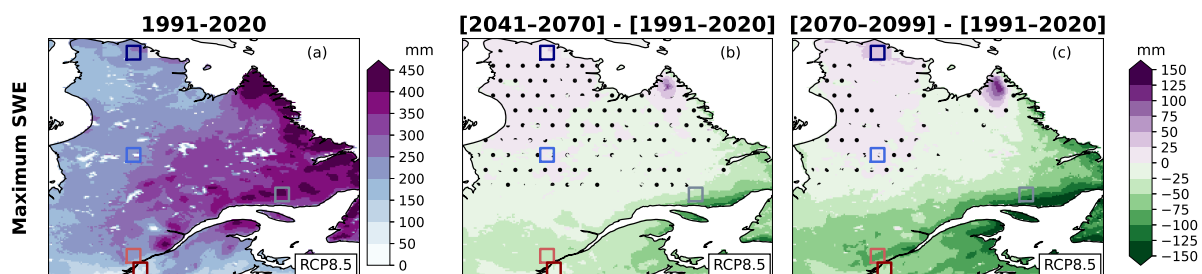


**Figure 4.** Annual maximum SWE for 1991–2020 (a), and differences between the 1991–2020 period and 2041–2070 (b) or 2070–2099 (c). Dotted areas are where less than 80 % of the simulations in the ensemble agree on the sign of change. Results are presented for the RCP8.5 ensemble.



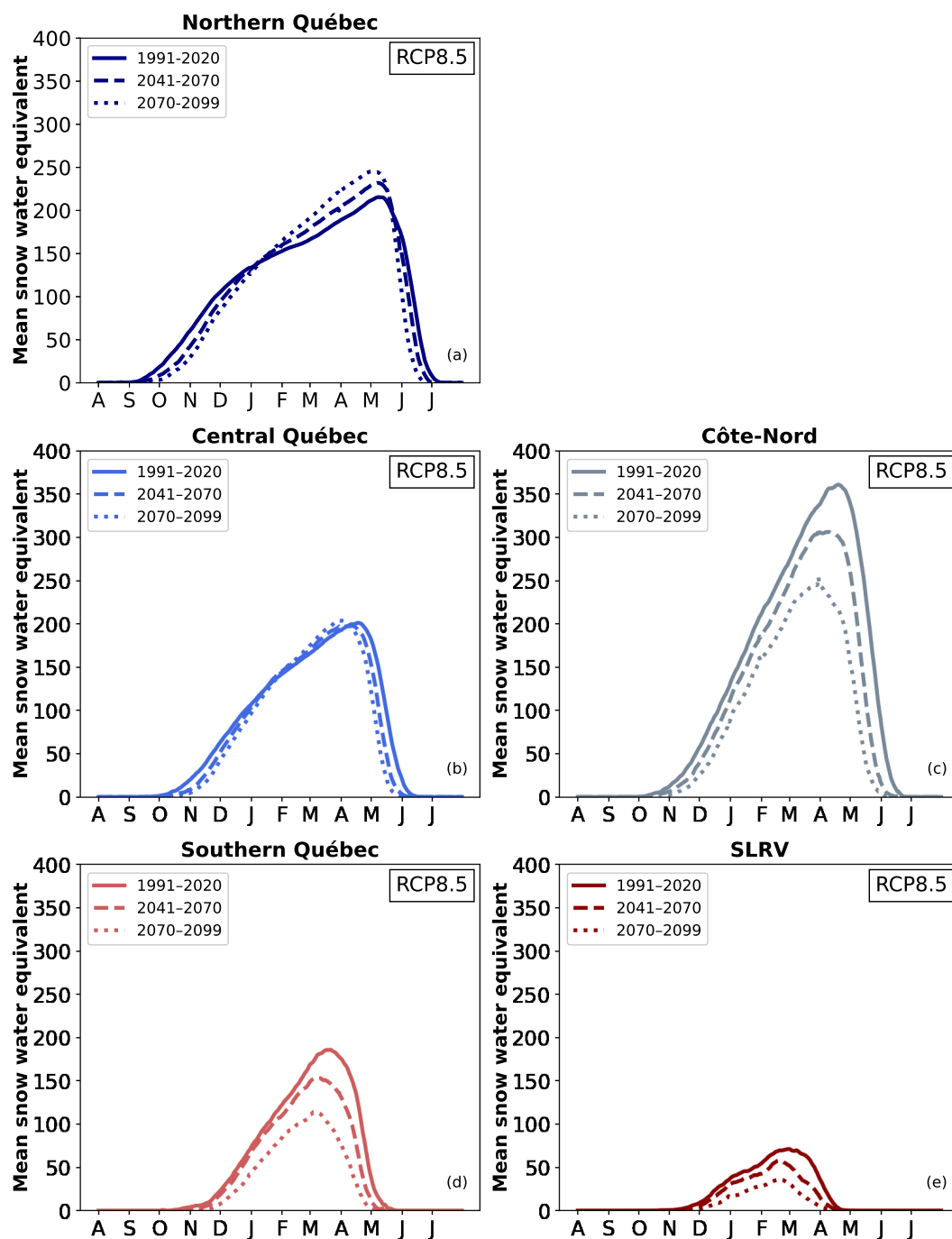


**Figure 5.** Annual cycle of SWE for the RCP8.5 ensemble in the five analysis regions.

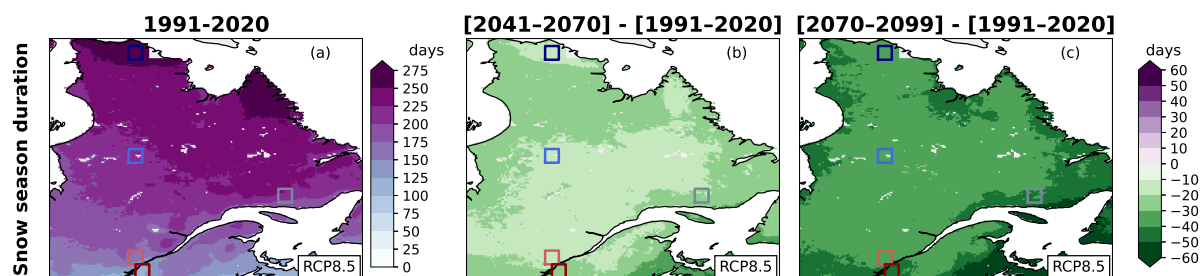


**Figure 6.** Annual snow season duration for 1991–2020 (a), and differences between the 1991–2020 period and 2041–2070 (b) or 2070–2099 (c). Dotted areas are where less than 80 % of the simulations in the ensemble agree on the sign of change. Results are presented for the RCP8.5 ensemble.

165 As time progressed, the magnitude of SWEmax increased in Nunavik and the Torngat Mountains, was stable for central Québec, and decreased for the other regions (Fig. 4, 5). More than 80 % of the simulations in the ensemble agreed on the sign of change in Nunavik, the Torngat Mountains, and the southern half of the domain. This change was consistent with the projected increase in precipitation and temperature in Québec (Bush and Lemmen, 2019). The timing of SWEmax also changed: the annual cycle of SWE showed that the maximum SWE occurred earlier (a change of about 6 to 10 days between  
 170 1991–2020 and 2070–2099) for four regions (Fig. 5a-d), while the signal was more ambiguous for the SLRV region (Fig. 5e).

The annual SWE cycle also showed a decrease in the duration of the snow season (Fig. 5). The change in SSD was almost spatially homogeneous, with a decrease of about 0 to -20 days [-20 to -50] for 2041–2070 [2070–2099] relative to 1991–2020 (Fig. 6). More than 80 % of the simulations in the ensemble agreed with the decrease. The SSD shrinkage was quite symmetrical as presented in the changes in SSS and SSE, except for the northern part of Québec (Fig. 3, 7). In this region, the  
 175 change in the snow season start was larger than the change in the snow season end but never exceeded 15 days (Fig. 7g,h). This change was more significant for 2070–2099 than for 2041–2070. This can be related to the iso-0 °C line moving northward. A large part of the domain experimented a warming that affected the snow season limits (SSS and SSE), but this warming was weaker in the northern part of Québec for these moments of the year, especially at the end of the season during the months of May and June (e.g. Leduc and Logan, 2025). The phenomenon may also explain why the end of the snow season for the  
 180 Côte-Nord region became closer to the one of central Québec as time passed (Fig. 3).

Over time, noSC increased by approximately 0 to +20 [+20 to +50] days for 2041–2070 [2070–2099] (Fig. 8). The spatial pattern of noSC was preserved for all periods. This increase in noSC could be the result of 1) the shrinkage of the snow season (Fig. 6); 2) changes in the distribution of days without snow cover during the snow season. To investigate the second point, we used the noSCseq indicator presented previously. Figure 9 shows the day of the year (angle) and the average length of  
 185 noSCseq starting on that day (radius), superposed on the mean snow season (white area) for each 30 year period. During the historical period, fragmentation rarely occurs during January or February, except in the SLRV region. No changes in January and February were projected for the northern and central Québec regions (Fig. 9a-f). For the other regions, the number of days with a noSCseq increased in January and February. The projected increase in temperature may explain the presence of noSCseq

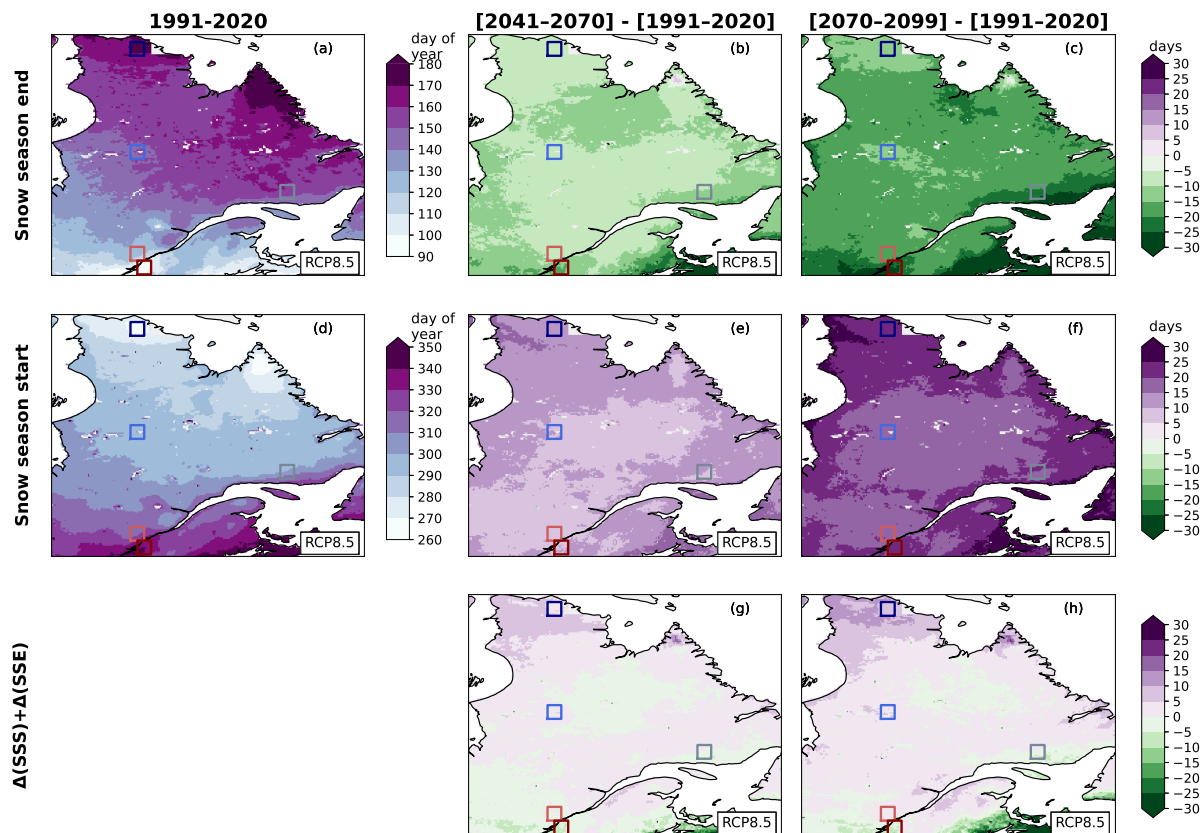


**Figure 7.** Snow season end (top), snow season start (middle) and the sum of the change in timing of snow season start and change in timing of snow season end (bottom), for 1991–2020 (left), and differences between the historical period (1991–2020) and 2041–2070 (centre) and 2070–2099 (right). Results are presented for the RCP8.5 ensemble.

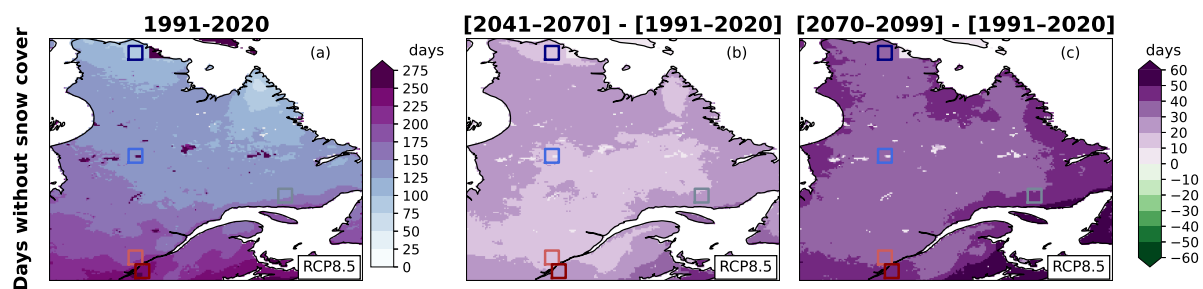


**Figure 8.** Annual days without snow cover for 1991–2020 (a), and differences between the 1991–2020 period and 2041–2070 (b) or 2070–2099 (c). Dotted areas are where less than 80 % of the simulations in the ensemble agree on the sign of change. Results are presented for the RCP8.5 ensemble.

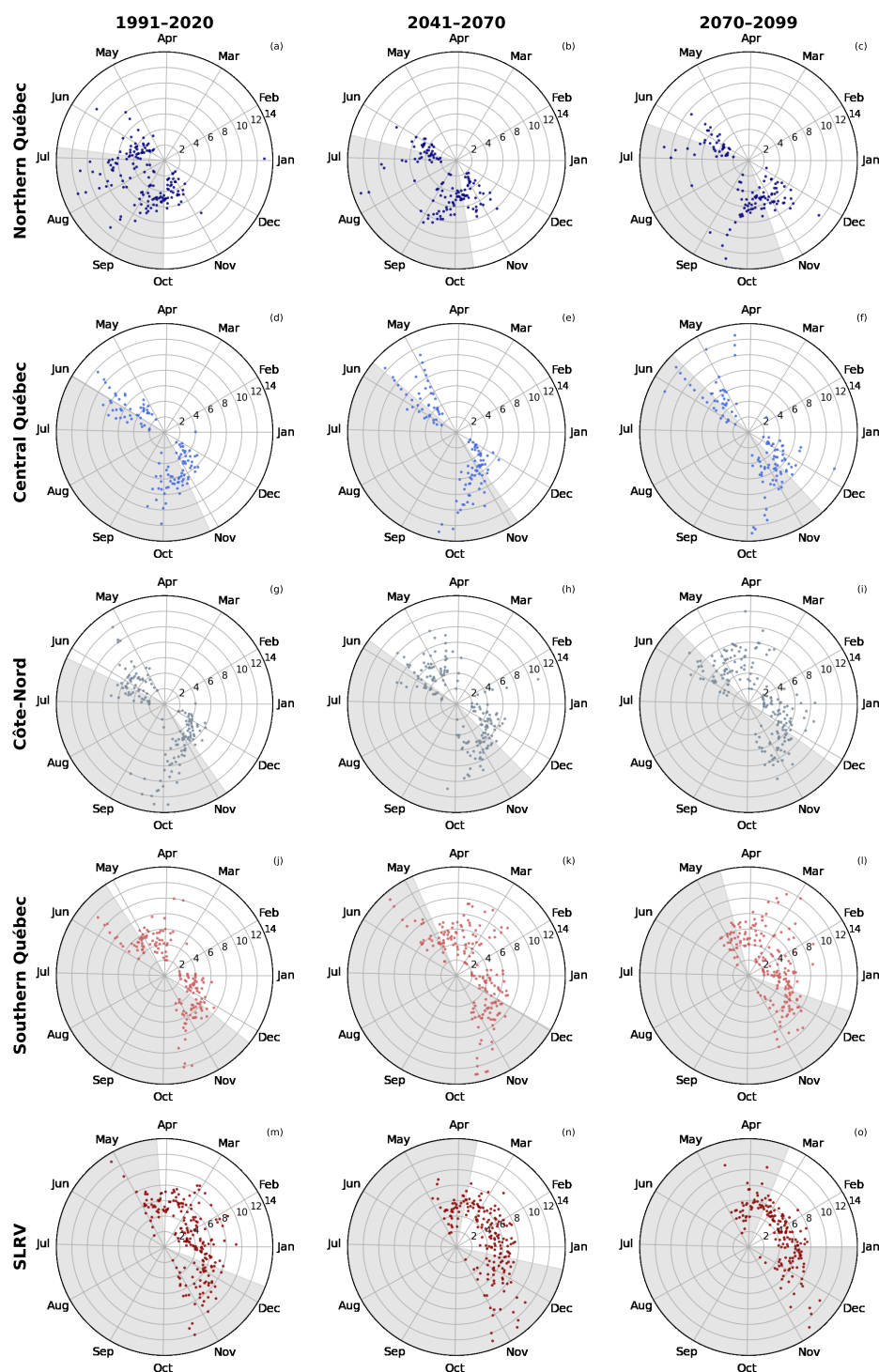


**Figure 9.** Length of sequences of 2 to 13 consecutive days without snow cover (radius) as a function of the day of the year (angle) for the RCP8.5 ensemble. The white part of each figure is the mean snow season for the studied period and region. The months are labelled at the first day of the month. Results are presented per region (rows) and for 1991–2020 (left), 2041–2070 (centre) and 2070–2099 (right).



in January and February for the Côte-Nord, southern Québec, and SLRV regions. As already shown, the season shortened, so  
 190 this result was expected. The noSCseq indicator has been classified into three categories according to the sequence length and  
 presented in Fig. 10 for each region. The calculation was performed for noSCseq during the mean snow season. During the  
 historical period, there were significant differences in the total number of noSCseq per region: from  $\approx 15$  noSCseq for the  
 central Québec region to  $\approx 45$  noSCseq for SLRV region. The proportion of noSCseq as a function of the length of the noSWE  
 sequence on the other hand presented no significant differences between regions: from 47 to 55 % for 2 to 5 consecutive days,  
 195 from 34 to 39 % for 5 to 10 consecutive days and from 10 to 15 % for more than 10 consecutive days. As time passed, no  
 significant changes arose in both the number of noSCseq during the snow season and the distribution of the three categories of  
 noSCseq (Fig. 10). As a consequence, the increasing of noSC seemed to be mainly related to the shrinkage of the snow season  
 and regions in the south of the domain (southern Québec and SLRV) presented more fragmentation during the snow season  
 than the other regions, whatever the period and the RCP ensemble considered.

## 200 4 Discussion

### 4.1 Comparison between RCP ensembles and simulations

All figures shown before are available for the RCP4.5 ensemble in Supplemental Material (SM). In general, trends are similar  
 for both ensembles, with more important changes for the RCP8.5 ensemble than for RCP4.5. The RCP4.5 ensemble has fewer  
 sequences of consecutive days without SWE than the RCP8.5. All this can be related to a smaller warming in the RCP4.5  
 205 ensemble, as expected.

When simulations are individually analyzed, different spatial patterns can be noted but as presented before in Fig. 7 and 8,  
 there is a good agreement between them regarding the trends (see SM) regardless of the RCP ensemble. However, this does  
 not apply to SWEmax where a larger spread between members is seen for both ensembles with large regions where less than  
 80 % of the members agree on the sign of change.

### 210 4.2 Selection criteria

The selection criteria presented in Sect. 2.3.2 leads to the rejection of all regional simulations driven by CanESM2, regardless  
 of the member (Tab.S1 in SM). This can be related to the warm bias of the CanESM2 model in eastern Canada. This bias leads  
 to less snowfall and more ablation of the snow cover. In Sheffield et al. (2013), the near-surface temperature bias for CanESM2  
 is presented for the eastern North-America (ENA) domain as described in Giorgi and Francisco (2000). This domain is similar  
 215 to the domain considered here for the simulation selection with an extension to the South, and the same northern border (i.e. the  
 50th parallel north). For that domain, the aforementioned study shows that CanESM2 has large warm biases for near-surface  
 temperature, regardless of the season, compared to observations for the 1979–2005 period (ENA: 4.79 °C in winter and of  
 3.4 °C in summer).

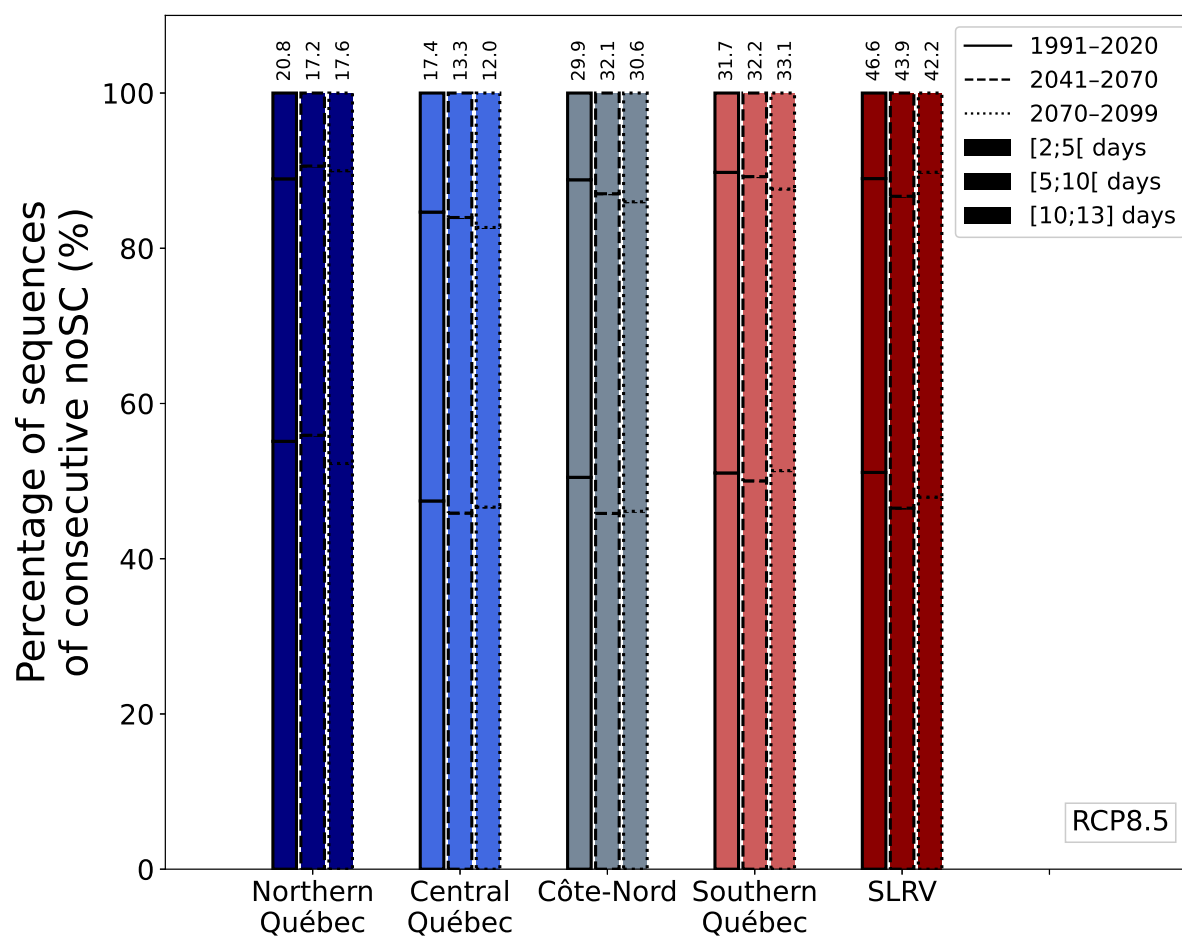


**Figure 10.** Percentage of noSCseq during the snow season for the historical period 1991–2020 (lines), 2041–2070 (dashed lines) and 2070–2099 (dotted lines) for the five regions of interest. Three duration ranges are presented with different transparencies: [2;5[, [5;10[ and [10;13] consecutive days for the RCP8.5 ensemble. Values on the top of each bar correspond to the total number of noSCseq during the snow season for each region and period.





Sheffield et al. (2013) also show the near-surface temperature biases for GFDL-ESM2M and HadGEM2-ES, and for another domain, Northeast Canada (NEC), which covers the northern part of the province of Québec. There, CanESM2 has a near-surface temperature bias of 3.13 °C in winter and 3.17 °C in summer. GFDL-ESM2M and HadGEM2-ES have greater biases in the NEC domain for near-surface winter temperatures (respectively 5.75 and -5.12 °C) than in the ENA domain (1.35 and -1.61 °C). Such differences in the near-surface temperature biases highlight the fact that the extent of the selection domain has to be carefully chosen and can be a limitation of the present study.

### 4.3 Indices defined with a threshold

In the list of indices analyzed in this study, only SWE<sub>max</sub> did not depend on a threshold. The other ones were conditional to the presence/absence of a snow cover, which was defined here as when  $SWE \geq 4$  mm. First, the choice of the threshold itself for the snow cover definition was somewhat arbitrary. Depending on the literature on which we rely, the snow cover threshold can have different values: 1 mm (Brown et al., 2010), 2.54 mm (0.1 in.) (McCrary and Mearns, 2019), 4 mm (Mudryk et al., 2017), or 5 mm (Brutel-Vuilmet et al., 2013). A sensitivity study to different thresholds would be of interest in future work but was not within the scope of the present article. Secondly, even if it was shown above that ERA5-Land performs better than other products for our studied domain and for SWE, it still has biases that could impact the statistical bias adjustment. For example, Leduc and Logan (2025) highlighted that the warm bias of daily minimum near-surface temperatures in ERA5-Land induces a bias in the climatology of the freeze-thaw events, which they define as a day where minimum temperature is below 0 °C and maximum temperature is above 0 °C. As a consequence, that study carried on with another reference for the statistical bias adjustment to avoid the bias in daily minimum near-surface temperatures in ERA5-Land. Here, such a bias could also have an effect on the SWE.

## 5 Conclusions

Snow cover is an important parameter for the evolution of climate in Canada. It has effects on ecology, agriculture, and many sectors of activity. Stakeholders and decision makers need useful data that is easily accessible and stored in a convenient format. In this study, we produced a portrait of useful snow cover indices for the Québec region. To achieve this result, we selected regional climate model simulations, applied a statistical bias adjustment to the simulated SWE, computed snow cover indices, and analyzed them. The overview of the snow cover change in northeastern Canada shows a shortening in the snow season, with similar, symmetrical changes for both the start and the end of the season, as well as a decrease of the maximum of SWE everywhere, except in the northernmost part of Québec (Nunavik and Torngat Mountains). The Côte-Nord, southern Québec and SLRV regions experiment a more fragmented snow season (consecutive days without snow cover during the season) than the northern and central Québec regions. These results agree with the literature (e.g. McCrary et al., 2022; Brown and Mote, 2009; Mudryk et al., 2020; Shi and Wang, 2015).

This study suffers a few limitations: the selection criterion is sensitive to the domain, the resulting ensemble of simulations is quite small and the SWE threshold used to define snow cover is somewhat arbitrary. The use of an external snow model



could have been an alternative to produce this data by considering all regional climate model simulations that have archived the required variables. The choice was made to use SWE simulated with the land surface model coupled to regional climate models in an attempt to preserve the physical interactions and feedback between atmospheric and surface variables. The application of a bias adjustment has impacted these interactions, but as only SWE was studied; this did not affect the results. A follow-up study could be useful to investigate the difference between our results and those produced with different land surface models in offline-mode using atmospheric input from the same regional climate simulations. This study could be extended to other regions. Precautions will have to be taken for mountainous regions like the Rocky Mountains, as the focus of the article was northeastern Canada which has a lower topography than western Canada. SWE behaviour in mountainous regions in regional climate models as well as in reanalyses can present some challenges.

**Code and data availability.** The datasets for both the daily timeseries and annual indices, the source code to produce these and some documentation are available at <https://doi.org/10.5281/zenodo.16422789>.

The datasets are also made available on Ouranos' PAVICS THREDDS server. A few indices not discussed here are also included in this folder. The indices computed over ERA5-Land are also available in another folder.

ERA5-Land data can be obtained from the Climate Data Store.

**CORDEX-NA data can be obtained from the project's website. Additional MRCC5 simulations from Ouranos are available upon request.**

**Author contributions.** ÉB conceptualized the study, designed the experimental setup, performed the analysis and prepared the manuscript with contributions from all co-authors; ÉD performed and improved the experimental framework; PB provided technical expertise and support; ÉD and PB curated the data.

**Competing interests.** No competing interests were reported by the authors.

**Acknowledgements.** We would like to thank Martin Leduc from Ouranos for his valuable and thoughtful insights, and review. We also thank Christine Penner for her linguistic review.

We acknowledge the World Climate Research Programme's Working Group on Regional Climate, and the Working Group on Coupled Modelling, former coordinating body of CORDEX and responsible panel for CMIP5. We also thank the climate modelling groups (listed in Tab. S1 in SM) for producing and making available their model output. We also acknowledge the Earth System Grid Federation infrastructure an international effort led by the U.S. Department of Energy's Program for Climate Model Diagnosis and Intercomparison, the European Network for Earth System Modelling and other partners in the Global Organization for Earth System Science Portals (GO-ESSP). We acknowledge the Quebec Ski Areas Association and the 2020-2025 action plan for responsible and sustainable tourism of the Ministry of Tourism of the government of Québec for funding this research.



## Funding

280 This study was funded by the Quebec Ski Areas Association and the government of Québec as a part of the 2020-2025 action plan for responsible and sustainable tourism of the Ministry of Tourism.

## ORCID

*Émilie Bresson* <https://orcid.org/0000-0002-5289-4937>; *Éric Dupuis* <https://orcid.org/0000-0001-7976-4596>; *Pascal Bourgault* <https://orcid.org/0000-0003-1192-0403>.



## 285 References

- Arora, V. K., Lima, A., and Shrestha, R.: The effect of climate change on the simulated streamflow of six Canadian rivers based on the CanRCM4 regional climate model, *Hydrology and Earth System Sciences*, 29, 291–312, <https://doi.org/10.5194/hess-29-291-2025>, 2025.
- Brown, R. D.: Analysis of snow cover variability and change in Québec, 1948–2005, *Hydrological Processes*, 24, 1929–1954, <https://doi.org/https://doi.org/10.1002/hyp.7565>, 2010.
- 290 Brown, R. D. and Mote, P. W.: The Response of Northern Hemisphere Snow Cover to a Changing Climate, *Journal of Climate*, 22, 2124 – 2145, <https://doi.org/10.1175/2008JCLI2665.1>, 2009.
- Brown, R. D., Derksen, C., and Wang, L.: A multi-data set analysis of variability and change in Arctic spring snow cover extent, 1967–2008, *Journal of Geophysical Research Atmospheres*, <https://doi.org/10.1029/2010JD013975>, 2010.
- Brun, E., Vionnet, V., Boone, A., Decharme, B., Peings, Y., Valette, R., Karbou, F., and Morin, S.: Simulation of Northern Eurasian Local  
 295 Snow Depth, Mass, and Density Using a Detailed Snowpack Model and Meteorological Reanalyses, *Journal of Hydrometeorology*, 14, 203 – 219, <https://doi.org/10.1175/JHM-D-12-012.1>, 2013.
- Brutel-Vuilmet, C., Ménégoz, M., and Krinner, G.: An analysis of present and future seasonal Northern Hemisphere land snow cover simulated by CMIP5 coupled climate models, *The Cryosphere*, 7, 67–80, <https://doi.org/10.5194/tc-7-67-2013>, 2013.
- Bush, E. and Lemmen, D.: Canada’s Changing Climate Report, Government of Canada, Ottawa ON, 2019.
- 300 Bélanger, G., Rochette, P., Castonguay, Y., Bootsma, A., Mongrain, D., and Ryan, D. A. J.: Climate Change and Winter Survival of Perennial Forage Crops in Eastern Canada, *Agronomy Journal*, 94, 1120–1130, <https://doi.org/https://doi.org/10.2134/agronj2002.1120>, 2002.
- Cannon, A. J., Sobie, S. R., and Murdock, T. Q.: Bias Correction of GCM Precipitation by Quantile Mapping: How Well Do Methods Preserve Changes in Quantiles and Extremes?, *Journal of Climate*, 28, 6938–6959, <https://doi.org/10.1175/JCLI-D-14-00754.1>, 2015.
- Derksen, C., Burgess, D., Duguay, C., Howell, S., Mudryk, L. R., Smith, S., Thackeray, C., and Kirchmeier-Young, M.: Changes in snow,  
 305 ice, and permafrost across Canada; Chapter 5 in Canada’s Changing Climate Report, (ed.) E. Bush and D.S. Lemmen, Government of Canada, Ottawa, Ontario, 2019.
- Dudley, R., Hodgkins, G., McHale, M., Kolian, M., and Renard, B.: Trends in snowmelt-related streamflow timing in the conterminous United States, *Journal of Hydrology*, 547, 208–221, <https://doi.org/https://doi.org/10.1016/j.jhydrol.2017.01.051>, 2017.
- Dutra, E., Balsamo, G., Viterbo, P., Miranda, P., Beljaars, A., Schär, C., and Elder, K.: New snow scheme in HTESSEL: description and  
 310 offline validation, <https://doi.org/10.21957/98x9mrv1y>, 2009.
- Elias Chereque, A., Kushner, P. J., Mudryk, L. R., Derksen, C., and Mortimer, C.: A simple snow temperature index model exposes discrepancies between reanalysis snow water equivalent products, *EGUsphere*, 2024, 1–23, <https://doi.org/10.5194/egusphere-2024-201>, 2024.
- Fox-Kemper, B., Hewitt, H., Xiao, C., Adalgeirsdóttir, G., Drijfhout, S., Edwards, T., Golledge, N., Hemer, M., Kopp, R., Krinner, G., Mix, A., Notz, D., Nowicki, S., Nurhati, I., Ruiz, L., Sallée, J.-B., Slangen, A., and Yu, Y.: Ocean, Cryosphere and Sea Level Change. In *Climate Change 2021: The Physical Science Basis. Contribution of Working Group I to the Sixth Assessment Report of the Intergovernmental Panel on Climate Change* [Masson-Delmotte, V., P. Zhai, A. Pirani, S.L. Connors, C. Péan, S. Berger, N. Caud, Y. Chen, L. Goldfarb, M.I. Gomis, M. Huang, K. Leitzell, E. Lonnoy, J.B.R. Matthews, T.K. Maycock, T. Waterfield, O. Yelekçi, R. Yu, and B. Zhou (eds.)], Cambridge University Press, Cambridge, United Kingdom and New York, NY, USA, <https://doi.org/10.1017/9781009157896.011>, 2021.
- Giorgi, F. and Francisco, R.: Uncertainties in regional climate change prediction: A regional analysis of ensemble simulations with the  
 320 HADCM2 coupled AOGCM, *Climate Dyn.*, 16, 169–182, 2000.



- Giorgi, F., Jones, C., and Asrar, G. R.: L'expérience CORDEX: répondre aux besoins d'information climatologique à l'échelle régionale, *Bulletin de l'OMM*, 58, 175–183, 2009.
- Hersbach, H., Bell, B., Berrisford, P., Hirahara, S., Horányi, A., Muñoz-Sabater, J., Nicolas, J., Peubey, C., Radu, R., Schepers, D., Simmons, A., Soci, C., Abdalla, S., Abellan, X., Balsamo, G., Bechtold, P., Biavati, G., Bidlot, J., Bonavita, M., De Chiara, G., Dahlgren, P., Dee, D., Diamantakis, M., Dragani, R., Flemming, J., Forbes, R., Fuentes, M., Geer, A., Haimberger, L., Healy, S., Hogan, R. J., Hólm, E., Janisková, M., Keeley, S., Laloyaux, P., Lopez, P., Lupu, C., Radnoti, G., de Rosnay, P., Rozum, I., Vamborg, F., Villaume, S., and Thépaut, J.-N.: The ERA5 global reanalysis, *Quarterly Journal of the Royal Meteorological Society*, 146, 1999–2049, <https://doi.org/https://doi.org/10.1002/qj.3803>, 2020.
- 325 Hoegh-Guldberg, O., Jacob, D., Taylor, M., Bindi, M., Brown, S., Camilloni, I., Diedhiou, A., Djalante, R., Ebi, K., Engelbrecht, F., Guiot, J., Hijioka, Y., Mehrotra, S., Payne, A., Seneviratne, S., Thomas, A., Warren, R., and Zhou, G.: Impacts of 1.5°C Global Warming on Natural and Human Systems. In: *Global Warming of 1.5°C. An IPCC Special Report on the impacts of global warming of 1.5°C above pre-industrial levels and related global greenhouse gas emission pathways, in the context of strengthening the global response to the threat of climate change, sustainable development, and efforts to eradicate poverty*[Masson-Delmotte, V., P. Zhai, H.-O. Pörtner, D. Roberts, J. Skea, P.R. Shukla, A. Pirani, W. Moufouma-Okia, C. Péan, R. Pidcock, S. Connors, J.B.R. Matthews, Y. Chen, X. Zhou, M.I. Gomis, E. Lonnoy, T. Maycock, M. Tignor, and T. Waterfield (eds.)], Cambridge University Press, Cambridge, United Kingdom and New York, NY, USA, <https://doi.org/10.1017/9781009157940.005>, 2018.
- 330 Kanda, N. and Fletcher, C. G.: Evaluating a hierarchy of bias correction methods for ERA5-Land SWE across Canada, *Environmental Research Communications*, <http://iopscience.iop.org/article/10.1088/2515-7620/aded5a>, 2025.
- Kouki, K., Räisänen, P., Luojus, K., Luomaranta, A., and Riihelä, A.: Evaluation of Northern Hemisphere snow water equivalent in CMIP6 models during 1982–2014, *The Cryosphere*, 16, 1007–1030, <https://doi.org/10.5194/tc-16-1007-2022>, 2022.
- 340 Lavoie, J., Caron, L.-P., Logan, T., and Barrow, E.: Canadian climate data portals: A comparative analysis from a user perspective, *Climate Services*, 34, 100 471, 2024.
- Leduc, M. and Logan, T.: The impact of climate change on the annual cycle of freeze-thaw events in eastern North America, *Journal of Applied Meteorology and Climatology*, submitted, 2025.
- 345 Lee, W., Gim, H., and Park, S.: Parameterizations of Snow Cover, Snow Albedo and Snow Density in Land Surface Models: A Comparative Review, *Asia-Pac J Atmos Sci*, 60, 185—210, <https://doi.org/https://doi.org/10.1007/s13143-023-00344-2>, 2024.
- Mankin, J. S., Viviroli, D., Singh, D., Hoekstra, A. Y., and Diffenbaugh, N. S.: The potential for snow to supply human water demand in the present and future, *Environmental Research Letters*, 10, 114 016, <https://doi.org/10.1088/1748-9326/10/11/114016>, 2015.
- Martynov, A., Laprise, R., Sushama, L., Winger, K., Šeparović, L., and Dugas, B.: Reanalysis-driven climate simulation over CORDEX North America domain using the Canadian Regional Climate Model, version 5: Model performance evaluation, *Climate Dynamics*, <https://doi.org/10.1007/s00382-013-1778-9>, 2013.
- 350 Matiu, M. and Hanzer, F.: Bias adjustment and downscaling of snow cover fraction projections from regional climate models using remote sensing for the European Alps, *Hydrology and Earth System Sciences*, 26, 3037–3054, 2022.
- McCrary, R. R. and Mearns, L. O.: Quantifying and diagnosing sources of uncertainty in midcentury changes in North American snowpack from NARCCAP, *Journal of Hydrometeorology*, 20, 2229–2252, 2019.
- 355 McCrary, R. R., Mearns, L. O., Hughes, M., Biner, S., and Bukovsky, M. S.: Projections of North American snow from NA-CORDEX and their uncertainties, with a focus on model resolution, *Climatic Change*, 170, 1–25, 2022.



- Mearns, L., McGinnis, S., Korytina, D., Arritt, R., Biner, S., Bukovsky, M., Chang, H.-I., Christensen, O., Herzmann, D., Jiao, Y., Kharin, S., Lazare, M., Nikulin, G., Qian, M., Scinocca, J., and Winger, W.: The NA-CORDEX dataset, version 1.0. NCAR Climate Data Gateway, Boulder CO., <https://doi.org/https://doi.org/10.5065/D6SJ1JCH>.
- Melton, J. R., Arora, V. K., Wisernig-Cojoc, E., Seiler, C., Fortier, M., Chan, E., and Teckentrup, L.: CLASSIC v1.0: the open-source community successor to the Canadian Land Surface Scheme (CLASS) and the Canadian Terrestrial Ecosystem Model (CTEM) – Part 1: Model framework and site-level performance, *Geoscientific Model Development*, 13, 2825–2850, <https://doi.org/10.5194/gmd-13-2825-2020>, 2020.
- Michel, A., Aschauer, J., Jonas, T., Gubler, S., Kotlarski, S., and Marty, C.: SnowQM 1.0: A fast R Package for bias-correcting spatial fields of snow water equivalent using quantile mapping, *Geoscientific Model Development Discussions*, 2023, 1–28, 2023.
- Molod, A., Takacs, L., Suarez, M., and Bacmeister, J.: Development of the GEOS-5 atmospheric general circulation model: Evolution from MERRA to MERRA2, *Geoscientific Model Development*, <https://doi.org/10.5194/gmd-8-1339-2015>, 2015.
- Morin, S., Samacoïts, R., François, H., Carmagnola, C. M., Abegg, B., Demiroglu, O. C., Pons, M., Soubeyroux, J.-M., Lafaysse, M., Franklin, S., Griffiths, G., Kite, D., Hoppler, A. A., George, E., Buontempo, C., Almond, S., Dubois, G., and Cauchy, A.: Pan-European meteorological and snow indicators of climate change impact on ski tourism, *Climate Services*, 22, 100215, <https://doi.org/https://doi.org/10.1016/j.cliser.2021.100215>, 2021.
- Mortimer, C., Mudryk, L. R., Cho, E., Derksen, C., Brady, M., and Vuyovich, C.: Use of multiple reference data sources to cross-validate gridded snow water equivalent products over North America, *The Cryosphere*, 18, 5619–5639, <https://doi.org/10.5194/tc-18-5619-2024>, 2024.
- Mudryk, L. R., Derksen, C., Kushner, P. J., and Brown, R. D.: Characterization of Northern Hemisphere snow water equivalent datasets, 1981–2010, *Journal of Climate*, <https://doi.org/10.1175/JCLI-D-15-0229.1>, 2015.
- Mudryk, L. R., Kushner, P. J., Derksen, C., and Thackeray, C.: Snow cover response to temperature in observational and climate model ensembles, *Geophysical Research Letters*, 44, 919–926, 2017.
- Mudryk, L. R., Santolaria-Otín, M., Krinner, G., Ménégot, M., Derksen, C., Brutel-Vuilmet, C., Brady, M., and Essery, R.: Historical Northern Hemisphere snow cover trends and projected changes in the CMIP6 multi-model ensemble, *The Cryosphere*, 14, 2495–2514, 2020.
- Mudryk, L. R., Mortimer, C., Derksen, C., Elias Chereque, A., and Kushner, P.: Benchmarking of SWE products based on outcomes of the SnowPEX+ Intercomparison Project, *EGUsphere*, 2024, 1–28, <https://doi.org/10.5194/egusphere-2023-3014>, 2024.
- Muñoz-Sabater, J., Dutra, E., Agustí-Panareda, A., Albergel, C., Arduini, G., Balsamo, G., Boussetta, S., Choulga, M., Harrigan, S., Hersbach, H., Martens, B., Miralles, D. G., Piles, M., Rodríguez-Fernández, N. J., Zsoter, E., Buontempo, C., and Thépaut, J.-N.: ERA5-Land: a state-of-the-art global reanalysis dataset for land applications, *Earth Syst. Sci. Data*, 13, 4349–4383, <https://doi.org/10.5194/essd-13-4349-2021>, 2021.
- Santolaria-Otín, M. and Zolina, O.: Evaluation of snow cover and snow water equivalent in the continental Arctic in CMIP5 models, *Clim Dyn*, 55, 2993–3016, <https://doi.org/https://doi.org/10.1007/s00382-020-05434-9>, 2020.
- Scott, D., Steiger, R., Knowles, N., and Fang, Y.: Regional ski tourism risk to climate change: An inter-comparison of Eastern Canada and US Northeast markets, *Journal of Sustainable Tourism*, 28, 568–586, <https://doi.org/10.1080/09669582.2019.1684932>, DOI: 10.1080/09669582.2019.1684932, 2020.





- Šeparović, L., Alexandru, A., Laprise, R., Martynov, A., Sushama, L., Winger, K., Tete, K., and Valin, M.: Present climate and  
 395 climate change over North America as simulated by the fifth-generation Canadian regional climate model, *Climate Dynamics*,  
<https://doi.org/10.1007/s00382-013-1737-5>, 2013.
- Sheffield, J., Barrett, A. P., Colle, B., Fernando, D. N., Fu, R., Geil, K. L., Hu, Q., Kinter, J., Kumar, S., Langenbrunner, B., Lombardo, K.,  
 Long, L. N., Maloney, E., Mariotti, A., Meyerson, J. E., Mo, K. C., Neelin, J. D., Nigam, S., Pan, Z., Ren, T., Ruiz-Barradas, A., Serra,  
 Y. L., Seth, A., Thibeault, J. M., Stroeve, J. C., Yang, Z., and Yin, L.: North American Climate in CMIP5 Experiments. Part I: Evaluation  
 400 of Historical Simulations of Continental and Regional Climatology, *Journal of Climate*, 26, 9209 – 9245, <https://doi.org/10.1175/JCLI-D-12-00592.1>, 2013.
- Shi, H. X. and Wang, C. H.: Projected 21st century changes in snow water equivalent over Northern Hemisphere landmasses from the CMIP5  
 model ensemble, *The Cryosphere*, 9, 1943–1953, <https://doi.org/10.5194/tc-9-1943-2015>, 2015.
- Themeßl, M. J., Gobiet, A., and Heinrich, G.: Empirical-Statistical Downscaling and Error Correction of Regional Climate Models and Its  
 405 Impact on the Climate Change Signal, *Climatic Change*, pp. 449–468, <https://doi.org/10.1007/s10584-011-0224-4>, 2012.
- Verseghy, D. L.: Class—A Canadian land surface scheme for GCMS. I. Soil model, *International Journal of Climatology*, 11, 111–133,  
<https://doi.org/https://doi.org/10.1002/joc.3370110202>, 1991.
- Vionnet, V., Mortimer, C., Brady, M., Arnal, L., and Brown, R.: Canadian historical Snow Water Equivalent dataset (CanSWE, 1928–2020),  
*Earth Syst. Sci. Data*, 13, 4603–4619, <https://doi.org/10.5194/essd-13-4603-2021>, 2021.
- 410 Zimova, M., Mills, L. S., and Nowak, J. J.: High fitness costs of climate change-induced camouflage mismatch, *Ecology Letters*, 19, 299–307,  
<https://doi.org/https://doi.org/10.1111/ele.12568>, 2016.